Society of Petroleum Engineers

SPE-189292-STU

Pore Structure Analysis Using Subcritical Gas Adsorption Method

Manju Pharkavi Murugesu, Colorado School of Mines

This paper was prepared for presentation at the SPE International Student Paper Contest at the SPE Annual Technical Conference and Exhibition held in San Antonio, Texas, USA, 9-11 October 2017.

This paper was selected for presentation by merit of placement in a regional student paper contest held in the program year preceding the International Student Paper Contest.

Abstract

The oil and gas industry has been tapping into tight reservoirs with low permeability and porosity. This calls for methods to enhance our understanding of tight reservoirs, such as shale. A large percentage of gas in place in shale reservoirs is in the form of adsorbed gas on the surfaces of pores. The pores of shale reservoirs range from micro-, meso- to macropores. Small pores contribute to large surface area accessible for adsorption, emphasizing the importance of studying pore structure in nanoscale. Subcritical gas adsorption isauseful methodto characterize pore structures in nanoscale in terms of quantifying pore volume, determining the presence of micropores, predicting pore geometries and the accessible surface area for adsorption.

This paper discusses results obtained from running adsorption on samples of four different formations: Niobrara shale, Lokpanta oil shale, Hawaiian basaltic rock and Berea sandstone. Some of the results used to both qualitatively and quantitatively study pore structures are isotherm, pore size distribution and specific surface area. These results both affirm and debunk generalizations tied to certain formations. For instance, sandstone typically has large grains and this is confirmed by the zero micropores shown in both its isotherm and pore size distribution. On the contrary, some of the basaltic rocks are expected to have highspecific surface area due to its high clay content, yet the samples showed low specific surface area instead. This informs the lack of information available on the sample, thus, initiating more tests to understand other factors that may be causing low specific surface area. Moreover, Lokpanta oilshale does not have any external information provided, but the isotherms and pore size distribution help to intuitively grasp the image of the samples' pore structures. This paper illustrates how best to analyze and compare the experimental results.

Subcritical gas adsorption makes it easy to picture pore structures at nanoscale. Understanding pore structures, specific surface area available for adsorption and micropore volume for storage purposes is crucial for applications, such as carbon capture and storage (CCS).

Introduction

The industry's focus on exploration and production from shale reservoir calls for betterunderstanding of such reservoir. Shale is known to trap and store a large amount of hydrocarbon gas in adsorbed state (Kang 2011). The transport, storage and adsorption capacity of shale rocks, however, depend on its pore structures.

Traditionally, Mercury Intrusion Porosimetry (MIP) technique is used in the laboratory to measure pore structures of sandstone and carbonate, but this method is not applicable to pore widthssmaller than 3.6 nanometers (Kuila 2013). Unlike conventional sandstone, shale reservoirs with its low permeability consist of nano-scaled pore system.

Subcritical gas adsorption has proven useful in characterizing nano-scaled pores. The International Union of Pure and Applied Chemistry (IUPAC) defines adsorption as the enrichment of molecules at an interface, such as the interface between solid pores and gas molecules (Thommes et al 2015). This paper specifically discusses the use of subcritical gas adsorption, a phenomenon that takes place below the critical point of the fluid. Below the critical point at low-pressure environment, the attraction between solid and gas is purely based on physisorption (Anovitz 2015). Weak Van der Waals forces, created as a result of temporary polarization between the fluid and solid, forman interaction between solid and gas molecules. This technique has proven useful in the study of pore structure, such as the pores' specific surface area, volume and size distribution.

This paper outlines the method to effectively interpret an isotherm, as per suggested by the IUPAC technical report. Techniques have already been established to inverse isotherms into quantitative results, such as specific surface area and pore size distribution. The techniques, known as Brunauer–Emmett–Teller (BET) and Density Functional Theory (DFT),are explained under the theoretical background section (Thommes 2010, Rouquerol et al 2007). When putting different results together, one gets a clearer idea of a sample's pore structure. Pore structure is crucial to understand how fluid move and are stored in the formation. Adsorption itself is a direct interaction between the pore wall and the fluid. Understanding the mechanism could prove useful to further the study of rock fluid interaction in adsorbed state.

Moreover, it is almost impossible to generalize the pore structures of all shale rocks due to its intense heterogeneity, not only between different shale plays, but also within the same interval of shale play. The heterogeneity comes from several characteristics of a reservoir, such as total organic content (TOC), clay content and maturity level. In addition, the lithology may compose of various types of rock such as mudstone, limestone, dolomite and sandstone (Chalmers et al. 2012).Prior literature studies have been conducted on shale samples, describing the effects of rock heterogeneity originated from clay content, total organic content (TOC) and maturity level (Kuila 2013, Saidian et al 2016). Thus, it is not advisable to generalize pore structures of shale samples. It is important to broaden the application of subcritical gas adsorption to rocks other than shale formation in order to understand the various factors that shape pore sizes of a sample.

Experimental Procedure

The experiment is subcritical gas adsorption, where gas is adsorbed onto the samples' pore wall below the saturation pressure of the fluid. In adsorption terms, gas is known as adsorptive while the sample is known as adsorbent. A cryogenic temperature (E.g.77K for nitrogen) is maintained constant throughout the experiment. This temperature is close to the boiling temperature of nitrogen and such low temperature is crucial for maximum adsorption.

Subcritical adsorption is based on static volumetric method, as illustrated by IUPAC (Thommes et al 2015). Several instruments are available commercially for subcritical gas adsorption. The instruments used for results shown in this paper are Micromeritics ASAP 2020™ and Quantachrome's Quadrasorb EVO.

Sample preparation is an important component of the experiment. The samples could either be crushed into powder under mesh 40 or broken into chips (Kuila & Prasad 2013). Previous studies by Kuila and Prasad suggest crushing the samples as this reduces the length of travel into the pores and equilibrium time is reached at reasonable time. Equilibrium time is the time set for diffusion into pores to happen before given relative pressure is achieved (Kuila 2013). Hence, samples in pellets may not register the complete surface area of pores, as the path of travel and equilibrium time is longer. This may not apply to all types of rocks.

Fig. 1 shows the isotherms of crushed vs. pellets of Hawaiian basaltic rocks. Although the crushed sample may have adsorbed more gas, the specific surface area of pellets (9.819 m^2/g) is higher than crushed powder (6.629 m^2/g). This could be due to the texture of rock samples. Basaltic rocks are known to have sponge-like pores with large surface area. By crushing the rocks, the pores may be broken down into smaller pieces, hence losing its large surface area. The crushed powder, however, adsorbed a lot more gas as higher mass of crushed sample is used (Fig. 1). This confirms the need to do trial experiments with different preparation methodsfor each set of sample before choosing the suitable preparation method.

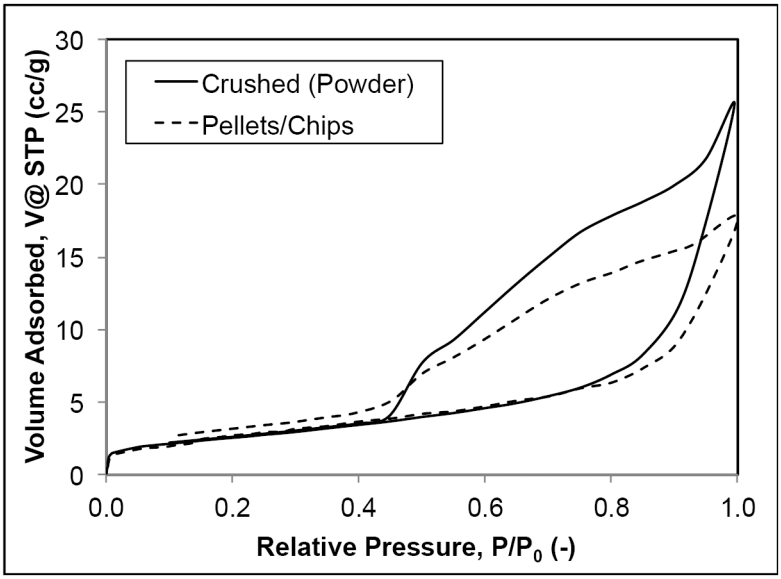

Figure 1—The isotherms of crushed vs. pellet Hawaiian basaltic rocks: the crushed sample adsorbed more volume of nitrogen gas than the pellets because higher mass of crushed sample is used; yet the specific surface area of pellet is higher.

The two main steps of subcritical adsorption is outgassing the sample and running adsorption analysis. Outgassing ensures removal of physically adsorbed unwanted vapors and gases from sample's internal and external surface (Sing et al 1985). Removing any vapors and volatile component ensures all of the pore walls to be in contact with the gas, except when organic mattersare blocking the pore throats. During degassing, sample cells, with crushed or pellet samples, are connected to degasser with a nitrogen backfill.Samplesare outgassed at a temperature of 200¼C for a minimum of 12 hours under vacuum of < 0.005 Torr/min (Kuila 2013). This is a standard procedure, but the length of time and temperature can vary depending on the sample. Too high of a temperature may do irreversible damage to the samples.

After degassing, the sample cells are transferred to adsorption analysis instrument. Volumetric method requires recording the volume of gas dosed into a calibrated known volume of sample cell containing the adsorbent. For this purpose, the dead volume of the sample cell with the adsorbent must be measured by dosing helium, a non-reactive gas. Then, the pressure slowly increases until saturation pressure of adsorptive fluid is reached. As the relative pressure (P/P_o) increases, the adsorptive is adsorbed onto the sample. The relative pressure changes from 0.03 to 0.995 at constant temperature. At desorption, the relative pressure is dropped from saturation pressure to almost P/P_o=0.05. Once these points are recorded, the instrument presents an isotherm of the material. A workflow of experimental procedure is shown in Fig 2. An isotherm shows the quantity of gas adsorbed at each relative pressure from adsorption to desorption as shown in Fig 3.

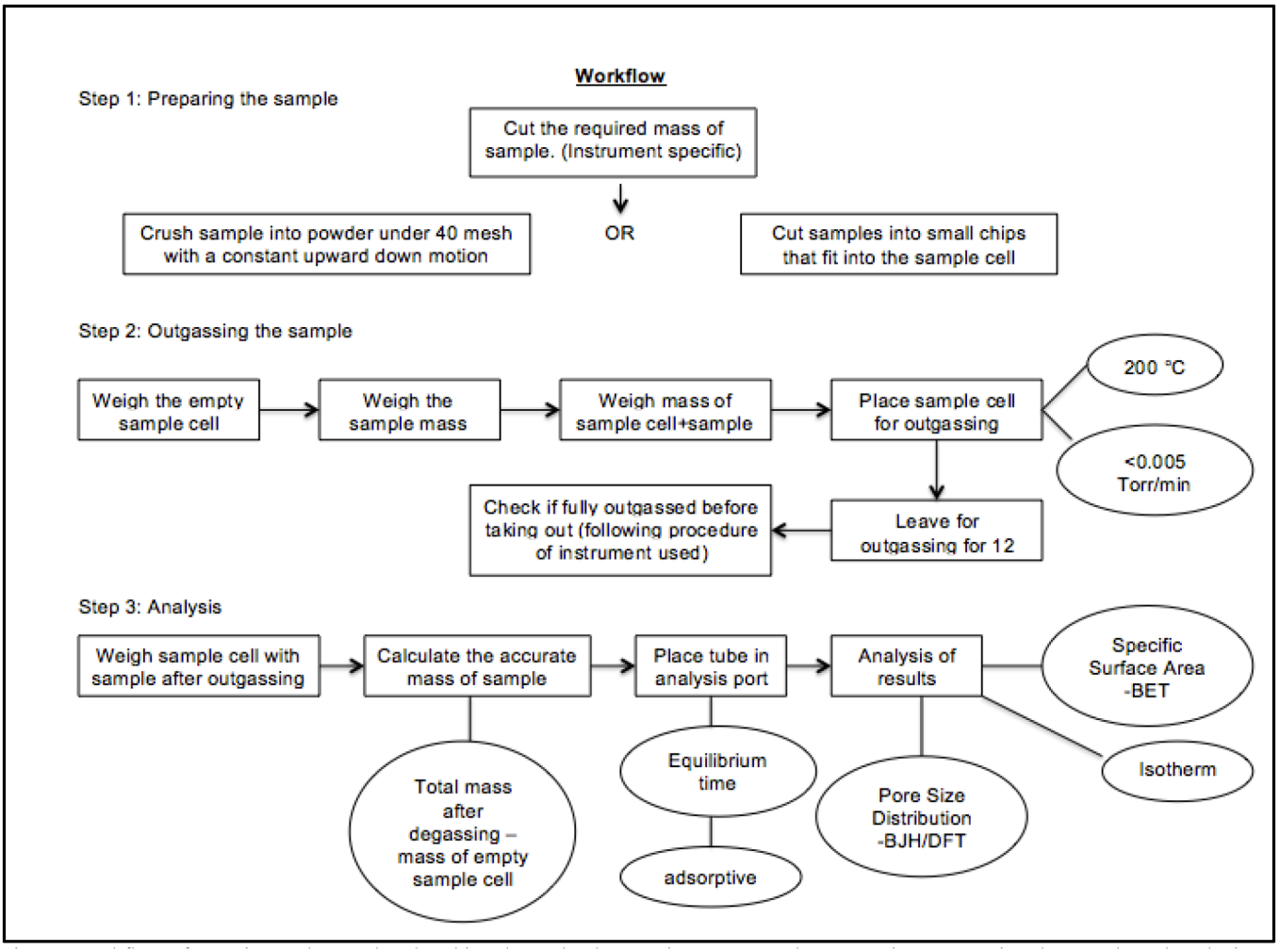

Figure 2—Workflow of experimental procedure breaking down the three main steps: sample preparation, outgassing the sample and analysis.

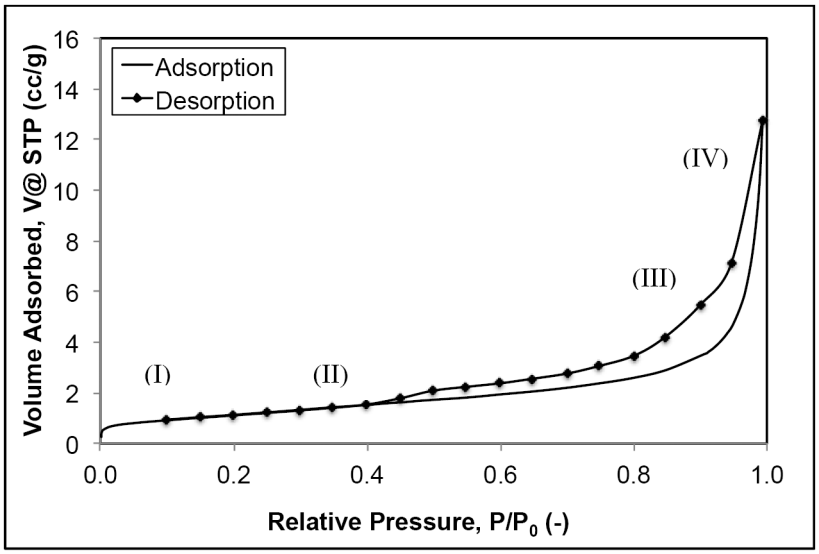

Figure 3—Isotherm of a sample: (I) micropore region; amount of gas adsorbed at low relative pressure correlates with the quantity of micropores; (II) monolayer adsorption; monolayer coverage before the inflection point; (III) mesopore filling; capillary condensation that leads to the formation of hysteresis (IV) macropore region; steeper curve indicating the presence of more macropores that are not imaged by the instrument.

Statement of Theory

Story behind isotherms

In a static volumetric method, adsorption and desorption are depicted by an isotherm (Fig. 3). Isotherms illustrate the resulting increase in volume of gas adsorbed as the pressure is increased up to the saturation pressure of fluid. Similarly, the adsorbed gas is released or desorbed from the adsorbent as the pressure is decreased from the saturation pressure. Isotherms are proven tools to qualitatively study the pore structures of adsorbents, especially the interaction between the solid and gas system. The shape of an isotherm qualitatively describes the relative amount of micro-, meso- and macropores, monolayer to multilayer adsorption and geometry of pores.

Micropores → < 2nm
Mesopores → 2nm – 50nm
Macropores → >50nm

I. Adsorption of any gas begins from the narrowest pores of an adsorbent. In subcritical gas adsorption, as the pressure is increased from near zero to the saturation pressure, the lowest pressures indicate the beginning of adsorption process. Instead of surface coverage, micropore filling takes place as a number of gas molecules completely fill up the 2nm width of micropores, a mechanism governed by the fluid-solid interaction (Storck et. al 1998, Sing et al 1985, Thommes & Cychosz 2014). The compactness of narrow pores leads to overlapping surface energy within the pores, leading to an enhanced fluid-rock attraction or adhesion forces (Sing et al 1985). Sing also explains the two types of micropore adsorption, where the primary micropore filling takes place with pore widths comparable to the size of gas molecules and secondary filling takes place at a slightly higher relative pressure. Therefore, the volume of gas molecules adsorbed at low relative pressures indicates the presence of micropore.

II. As micropores are filled, gas is also being adsorbed onto the adsorbent, forming a monolayer. The initial coverage of the surface is utilized by Brunauer, Emmett and Teller (BET) to determine the specific surface area accessible for adsorption. BET method takes into account that multilayers start forming even before the completion of the first layer (Rouquerol 2007). It is important to further the study of monolayer formation, as it is a direct illustration of fluid-solid interaction, especially the fluid affinity to the rock samples, in the case of shale reservoirs. From Fig 3, the linear region following micropore filling ending before the sharp inflection point at relative pressure (P/P_o=0.4) indicates monolayer adsorption (Kuila 2013).

III. As the pressure is increased towards saturation pressure, the formation of successive layers fills up the mesopores (2-50nm), causing capillary condensation. Due to capillary condensation, the gas molecules filling up the mesopores condense into its liquid form at a pressure below the saturation pressure, P_o of the bulk liquid (Lowell et. al 2012). This process depends largely on the cohesion forces between the fluid molecules itself. Interestingly, this process is the reason behind hysteresis between adsorption and desorption. As the pressure is decreased and desorption occurs, pore evaporation takes place at a pressure lower than pore condensation pressure (Lowell et. al 2012). The hysteresis loops are proven to be correlated to pore geometry and the correlations are shown as different hysteresis types by the International Union of Pure and Applied Chemistry (IUPAC) in 2015 (Sing et al 1985, Kuila 2013, Thommes et al 2015).

IV. Although there is no such phenomenon like micropore filling or pore condensation taking place at the macropores (>50nm), the presence of macropores can still be validated by isotherms. At high relative pressure (P/P_o=1.0), most of the micropores and mesopores are already filled. Thus, if a

plateau is observed at near saturation pressure, the adsorbent does not have macropores. Similarly, a steep slope P/P_o=1.0 verifies the presence of macropores (Sing et al 1985).

Inversion Methods

While isotherms qualitatively illustrate the pore structures of a solid adsorbent, methods have been established to inverse from experimental isotherm to quantitative methods, such as (i) pore size distribution, and(ii) specific surface area.

Pore Size Distribution. Typically, the Barrett–Joyner–Halenda (BJH) method has been prevalently used to determine pore size distribution. It is derived from modified Kelvin equations (Rouquerol et al 2013, Lowell et al 2012).

$$\ln\left(\frac{p}{p_0}\right) = -\frac{2\gamma V_m}{RT(r_p - t_c)} \quad (1)$$

The equation demonstrates gas-liquid phase transition of a bulk fluid. γ is surface tension, V_m is molar volume of liquid, r_p is pore radius and t_c is statistical thickness of multilayer (Lowell et al 2012, Sing et al 2015). The widely known BJH method applies accurately for mesoporous solids, yet it does not apply to narrow micropores, as BJH does not consider the curvature and surface forces in narrow pores (Lowell et al 2012). The limitation posed by classical Kelvin equation is overcome by applying a microscopic method, such as Density Functional Theory (DFT).

DFT takes into account the configuration of adsorbed layer in a molecular level, allowing us to study volume of gas adsorbed in micropores (Thommes 2010). Several kernels are available for DFT analysis. The kernel used for this specific analysis is the *QSDFT kernel on carbon with slit cylindrical pores on adsorption branch*. The different kernels are explained by IUPAC technical report in 2015. DFT pore size distribution falls within micro-mesoporous range. It shows the amount of micro- and mesopores relative to each other. Pore size distribution can be displayed in many manners. In this paper, differential pore volume (cc/g/nm) is used as the independent variable to better represent the micropores available in the adsorbent

Assessment of Specific Surface Area. The most commonly used inversion method to determine specific surface area is Brunauer-Emmett-Teller (BET) method. Specific surface area gives an estimated surface area of the rock, allowable for storage by adsorption in shale reservoirs. BET is a mathematical analysis that derives surface area of monolayer coverage observed in an isotherm (Rouquerol et al 2007). It is based on several assumptions as stated by Brunauer. One such assumption is monolayer coverage that occurs at P/P_o=0.05-0.35, where the BET plot ($P/n(p_o-p)$ vs. P/P_0) is linear with a positive intercept, C as shown by Rouquerol et al 2007. All of the specific surface area shown in Table 1 contains positive C intercepts, thus validating the specific surface areas obtained.Another assumption is the molecular cross sectional area used in the given BET equation. The molecules uniformly cover the surface of the adsorbent, but the BET specific surface area (a_s) varies depending on the molecular cross sectional area (σ_m) (Rouquerol et al 2007).

$$a_s(BET) = n_m * L * \sigma_m / m \quad (2)$$

(Thommes et al 2015)

Table 1—BET Specific Surface Area for two molecular cross sectional area: 16.2 Å and 13.5 Å.

Sample ID	Description	C- Constant	Specific Surface Area, SSA (m^2/g)	
			16.2 Å	13.5 Å
Pellet2005	Aluminum Silicate	180.66	95.739	79.783
BS3 - 2936'	Niobrara	13.627	2.424	2.02
BS3 - 3013'	Niobrara	79.297	2.651	2.209
BS3 - 3164'	Niobrara	53.837	7.278	6.002
BS3 - 3193.3'	Niobrara	23.321	3.511	3.115
HBR 524'	Hawaiian Basaltic Rocks	72.778	1.203	1.002
HBR 904'	Hawaiian Basaltic Rocks	202.103	6.924	5.77
HBR 924'	Hawaiian Basaltic Rocks	33.873	2.819	2.349
HBR 1058'	Hawaiian Basaltic Rocks	269.229	7.835	6.529
L3	Lokpanta Oilshale	43.479	10.748	8.957
L5	Lokpanta Oilshale	42.646	7.203	6.003
L10	Lokpanta Oilshale	49.366	2.256	1.88
L13	Lokpanta Oilshale	21.702	13.605	11.076
Berea	Sandstone	47.458	0.536	0.447

Due to nitrogen's quadrupole moment, it may have two different molecular cross sectional areas with widths of either 16.2Åor 13.5 Å. Both values are recorded to show the difference. The real surface area, hence could range anywhere between the two values.

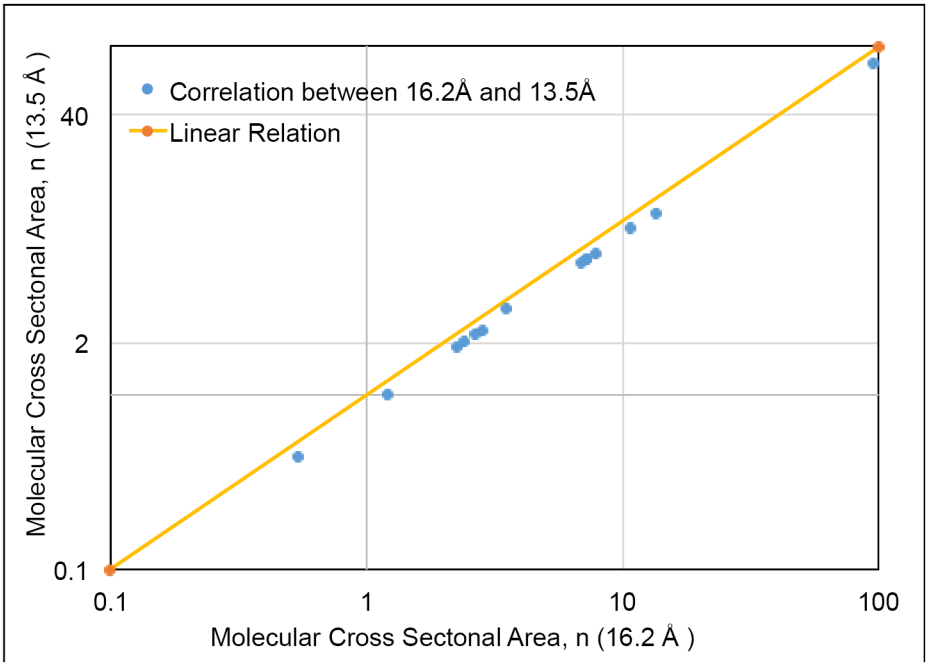

Figure 4—The linear relation between two different molecular cross sectional areas. The linear relation indicates that whether 13.5 Å or 16.2 Å is used for molecular cross sectional area, the result is considered reliable as long as one value is used consistently for a set of samples.

Data and Results

Among the many results that can be obtained from running adsorption (*see* Lowell et al), some that have been proven useful in characterizing pore textures are isotherms, pore size distribution and specific surface area. These results for different set of samples are presented in this section. Refer Table 2 for sample information.

Table 2—The available information on properties of samples run in subcritical adsorption analysis

Berea Sandstone

Samples ID	Porosity (-)	Permeability, k (mD)	Minerals
Berea SS	0.18	228	quartz, lithics, feldspar, kaolinite

Niobrara Shale

Samples ID	Description	Maturity Level	TOC (wt %)	T_{max} (°C)	Illite+Smectite Content (wt %)
BS3 - 2936'	A-chalk	Immature Oil	2.710	432.72	5
BS3 - 3013'	B-chalk	Mature Oil	2.305	439.69	8
BS3 - 3164'	D-chalk/marl	Immature Oil	0.640	349.65	11
BS3 - 3193.3'	Ft. Hays Limestone	Immature Oil	0.280	416.83	3

Hawaiian Basaltic Rocks

Samples ID	Porosity (-)	Cation Exchange Capacity, CEC (meq/100g)	Smectite Content (wt %)
HBR 524'	0.328	0.653	0
HBR 904'	0.077	11.36	1
HBR 924'	0.261	22.68	7
HBR 1058'	0.149	23.93	17

Lokpanta Oilshale

Samples ID	TOC (wt %)	T_{max} (°C)	Minerals
L3	2 to 7	430-441	quartz, calcite, mixed layer of illite-smectite, kaolinite
L5			
L10			
L13			

Standard Material: Alumina

With every test on a sample, a corresponding test is run on alumina, a standard sample provided by manufacturer with the expected isotherm and range of specific surface area (SSA). Fig. 5 shows that the laboratory test on alumina produces reliable result as it produces similar isotherm to the one provided by the manufacturer. Both isotherms reach monolayer coverage at relative pressure (P/P_o)=0.7. The hysteresis also rises linearly and stops abruptly at (P/P_o)=1.0, indicating the larger portion of macropores. The specific surface area of this sample is 95.739 m^2/g, which falls within the expected range of 98.71 (/7.53) m^2/g.

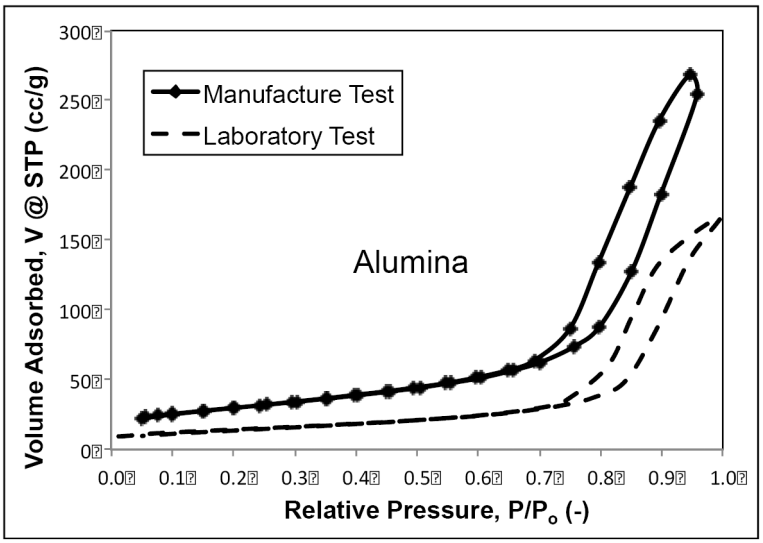

Figure 5—Subcritical nitrogen adsorption on alumina: the isotherm shape obtained for alumina is confirmed by manufacturer's test due to similar shapes. Notice the difference in nitrogen volume adsorbed compared to the manufacturer's test. This is due to the lower amount of sample used in the laboratory test.

Sandstone

Berea sandstone sample, obtained from the Appalachian basin, has good porosity and permeability (see Table 2). Subcritical adsorption starts from the narrowest pores at low pressure. Thus, the lack of gas adsorbed at the lowest relative pressure (Fig. 6) indicates zero micropores in this sample, which is confirmed by pore size distribution in Fig. 7. This sample has significant mesopores because the separation between adsorption and desorption happens as a result of pore condensation and evaporation that takes place in the mesoporous region. The amount of mesopores can be estimated from pore size distribution. The steep slope at saturation pressure shows that there may be more macropores. Typically, sandstone is known to contain significant macropores. Hence, the pore size distribution ranges from meso- to macropores. Fig. 7 illustrates significant amount of mesopores, but there may be more macropores that were not imaged by the instrument used. The resolution of subcritical adsorption instrument is limited to micro-mesoporous regions.

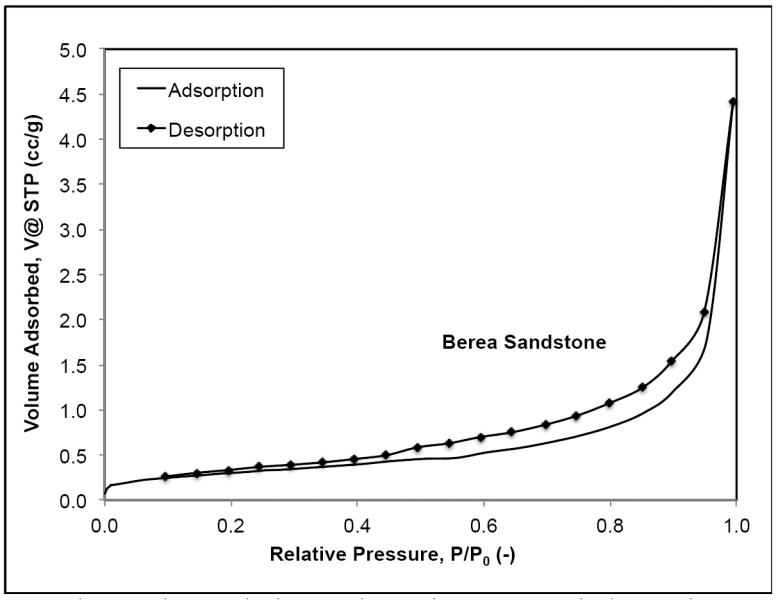

Figure 6—The isotherms of Berea Sandstone: The sample does not have micropores, yet the hysteresis suggests the presence of mesopores and the steep rise at the saturation point indicates macropores.

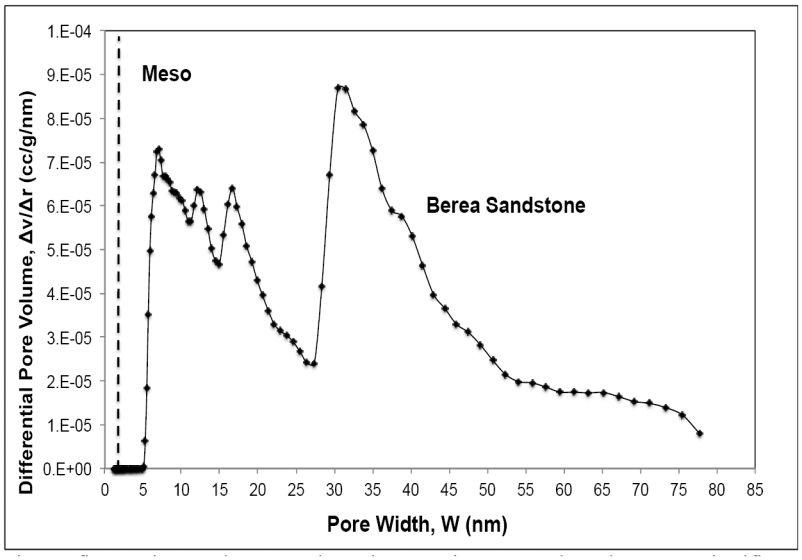

Figure 7—Pore Size Distribution: it confirms Fig. 6 because there is no micropores, but there are significant mesopores and some macropores.

Shale Rocks

Niobrara is a shale rock formation extending throughout northeast Colorado, Northwest Kansas, Southwest Nebraska and Southeast Wyoming. These samples are similar to samples studied by Al-Khalifa 2016. Fig. 8 shows the isotherms of four different samples obtained from marls and chalk intervals of Niobrara carbonate system of Denver basin. Fig. 8a, 8b, 8c and 8d all show similar shape of isotherms throughout the pressure rise and drop, including the hysteresis.

The theory behind isotherm allows prediction of micro-, meso- and macroporous region. Typically, shale samples are known to have significant amount of micropores. Adsorption accounts for large percentage of gas in place in a shale reservoir due to the high surface area provided by micropores (Ambrose et al 2012). However, all four Niobrara samples have zero to low volume of gas adsorbed at low relative pressure, indicating the low probability of having micropores. Thus, study of shale pore structures are important, yet direct association of shale reservoirs to high micropores must be avoided as it could also depend on other factors, such as total organic content (TOC), maturity and clay content. For example, Niobrara 3164' (Fig 8c) seems to have more volume of gas adsorbed at the low relative pressure compared to other samples. This is supported by the large TOC content of this sample. Organic content itself is known to contain pores that traps significant amount of gas (Kang et al 2011), confirmed by a high specific surface area of Niobrara 3164' as shown in Table 1 and the pore size distribution in Fig. 9.

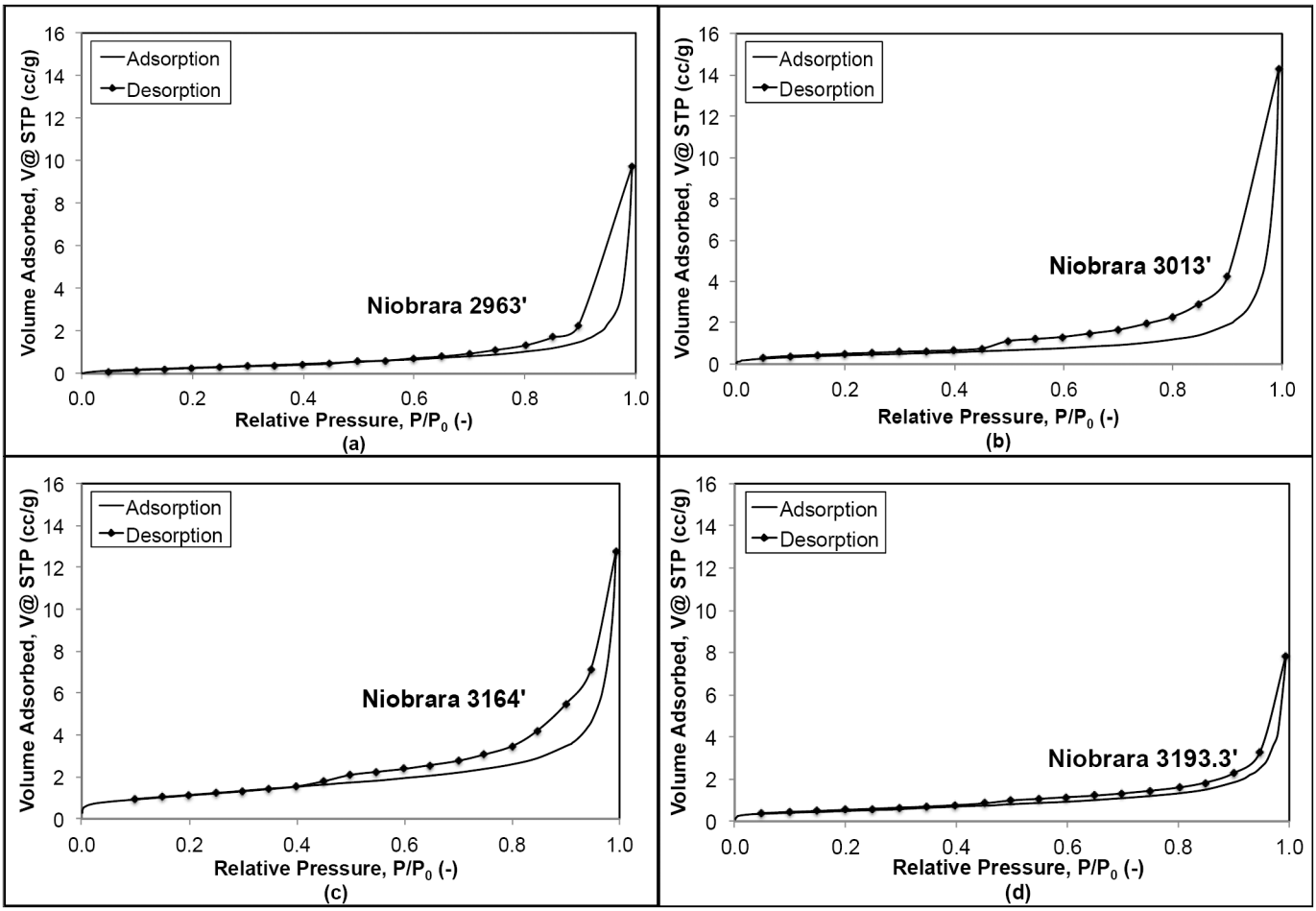

Figure 8—The isotherms of Niobrara samples: (a) A-chalk from immature oil window; (b) B-chalk from mature oil window; (c) D-chalk/marl from immature oil window with high clay content and low maximum temperature; (d) Ft. Hays Limestone from immature oil window with lowest TOC and clay content in this group of Niobrara samples. All samples have similarly shaped hysteresis type III for non-rigid aggregates of plate-like particles. They generally have low micropores due to the low amount of gas adsorbed at low relative pressure and suggest the presence of macropores with the large amount of gas adsorbed at high relative pressure.

At the mesoporous region, hysteresis of all four samples looks similar. Hysteresis is the result of difference in pore evaporation and condensation caused by pore textures (Thommes et al 2015). From correlations provided by IUPAC technical report in 2015, the shapes of hysteresis shown in Fig. 8 correlate with hysteresis type III for non-rigid aggregates of plate-like particles (Thommes et al. 2015). Despite using similar amount of samples, Niobrara 3193.3' has adsorbed lower amount of nitrogen than other samples with minimal separation between adsorption and desorption. This may be due to the weaker interaction between the pore wall and nitrogen fluid (Lowell et al 2012).

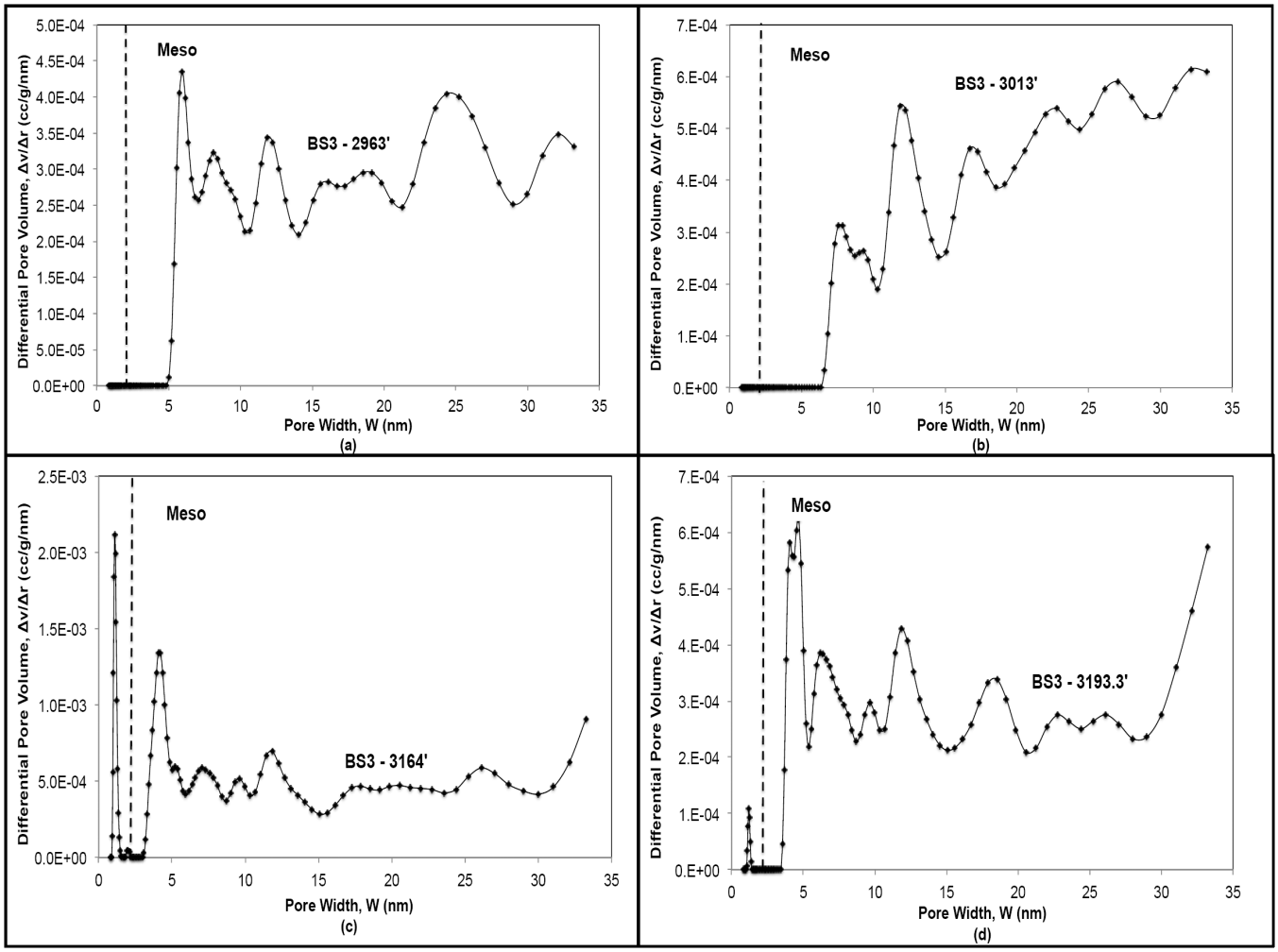

Figure 9—Pore size distribution of Niobrara samples using Density Functional Theory (DFT): (a) Niobrara 2963' has no micropores, but large amount of mesopores, (b) Niobrara 3013' does not have micropores, but shows an increasing trend of meso- and possibly macropores that was not imaged by microscopic DFT method, (c) Niobrara 3164' is dominated by micropores and the increasing trend at 33nm pore width shows it may have some macropores, (d) Niobrara 3193.3' has little micropores, large amount of mesopores and possibly more macropores.

The isotherms suggest presence of macropores due to the steep slope at P/P_o=1.0. Pore size distribution found through microscopic Density Functional Theory (DFT) images micro- to mesoporous scale, masking the exact amount of macropores. The presence of macropores, however, can be predicted by the ending trend at mesoporous region. If the trend is increasing, there may be more macropores in the samples, not imaged by DFT (refer Fig. 9).

Hawaiian Basaltic Rocks

A wellbore is drilled for the Humu'ula Groundwater Research Project in Hawaii. 28 core samples were obtained and run for surface area analysis. These are basaltic rocks from Humu'ula saddle region, located between Mauna Loa and Mauna Kea volcanoes of Hawaii. 4 samples were chosen for this study due to their distinct clay content, cation exchange capacity and porosity. Cation exchange capacity is sum of exchangeable cations that shows the surface energy of the pores (Chapman 1965). These properties may help us understand the isotherms and pore size distribution of these samples. One important feature of the basaltic rock is the absence of TOC and maturity. For more information on these rocks, refer to Revil et al 2016.

The isotherms indicate samples 1058' and 904' to have more micropores than samples 924' and 524' (Fig. 10). On the contrary, pore size distribution (Fig. 11) shows sample 524' to have micropores despite its

low specific surface area (Table 1). Therefore, this shows the lack of data to understand the presence of micropores. The shape of the hysteresis is indicative of hysteresis type III for non-rigid aggregates of plate-like particles (Thommes et al. 2015). Sample 904' and 1058' are also adsorbing a lot more nitrogen gas than the other samples. This is confirmed by the large specific surface area of these samples (refer Table 1). Clay content directly correlates with specific surface area, however, sample 904' does not have much clay content despite its high specific surface area. A deeper understanding of basaltic rock is necessary to further evaluate the behavior of these rocks' pore structure. The isotherms also suggest the presence of macropores due to the steep slope at P/P_o=1.0. More experiments, such as SEM images or FeSEM, may be needed to completely understand the basaltic rocks' texture.

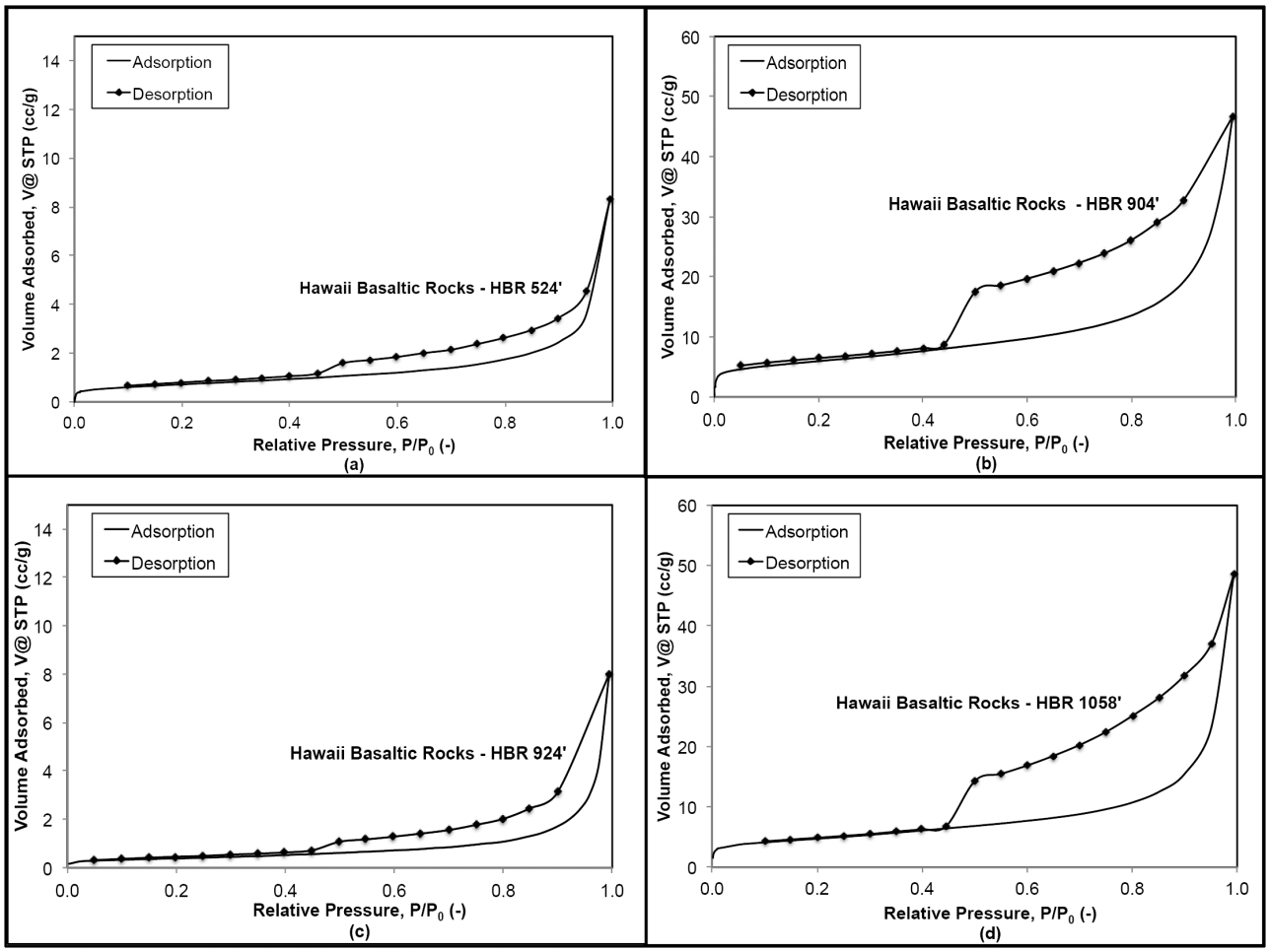

Figure 10—The isotherms of Hawaiian basaltic rock samples obtained from different depth. The numbers in the sample name refer to their depth: (a) HBR 524' has the highest porosity, but lowest clay content among all four samples; (b) HBR 904' has adsorbed some gas at low relative pressure, indicating the presence of micropores; (c) HBR 924' has high porosity, cation exchange capacity and some clay content, yet there are no micropores according to the isotherm; (d) HBR 1058' has the highest clay content and cation exchange capacity. All samples indicate the presence of macropores with the steep slope at saturation pressure.

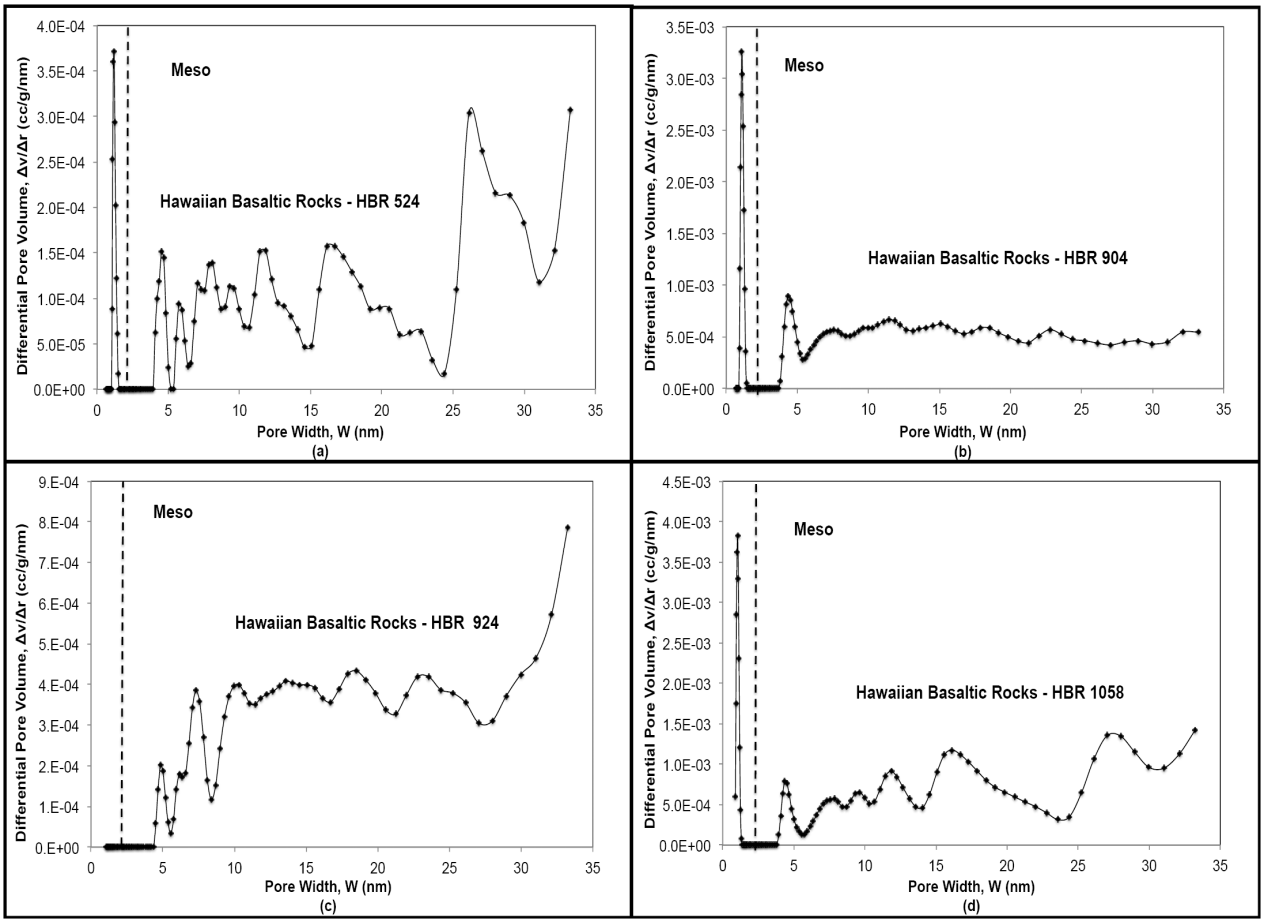

Figure 11—Pore size distribution of Hawaiian basaltic rocks: (a) HBR 524' has micropores, some mesopores and the rising trend after 30nm pore width indicates the possibility of macropores; (b) HBR 904' has micropores, but does not seem to have any meso- or macropores; (c) HBR 924' does not have micropores, but it has meso- and macropores; (d) HBR 1058' has micropores, no significant mesopores, but the rising trend after 30nm pore width may indicate some macropores.

Oil Shale

Generally, oil shale is organic rich, fine-grained sedimentary rocks. The samples are obtained from Lokpanta near Okigwe, close to the Lower Benue Trough, Nigeria. These samples are generally dark grey, laminated and mostly consist of Marlstone. The total organic content (TOC) of the samples ranges from 2 to 7 wt%. The maximum temperature for the oil shale of Lokpanta ranges from 430-441°C. Minerals in the raw form of these samples are mainly quartz, calcite, mixed layer of illite-smectite and kaolinite. The four samples ran for surface area analysis are labeled as L3, L5, L10 and L13.

Without any particular information on any one of these samples, looking at the result gives an intuitive idea of the pore structures. L3, L5, L10 and L13 from Fig 12 have low volume of nitrogen gas adsorbed at low relative pressure, indicating the minimal probability of having micropores. This is confirmed by the low level of micropores in the pore size distribution (refer Fig. 13). At the mesopore region, all four samples have similarly shaped hysteresis type III for non-rigid aggregates of plate-like particles to silt-shaped particles (Thommes et al. 2015). L13, however, has a larger hysteresis than other oilshale samples. Despite the lack of quantitative information, this allows marking L13 as being different than other samples. Hysteresis happens due to pore condensation, the larger gap suggests that it takes more pressure loss for pore evaporation to happen. For instance, nitrogen gas may still be condensed at the pore neck, blocking the path for gas from inside the pores from leaving in L13.

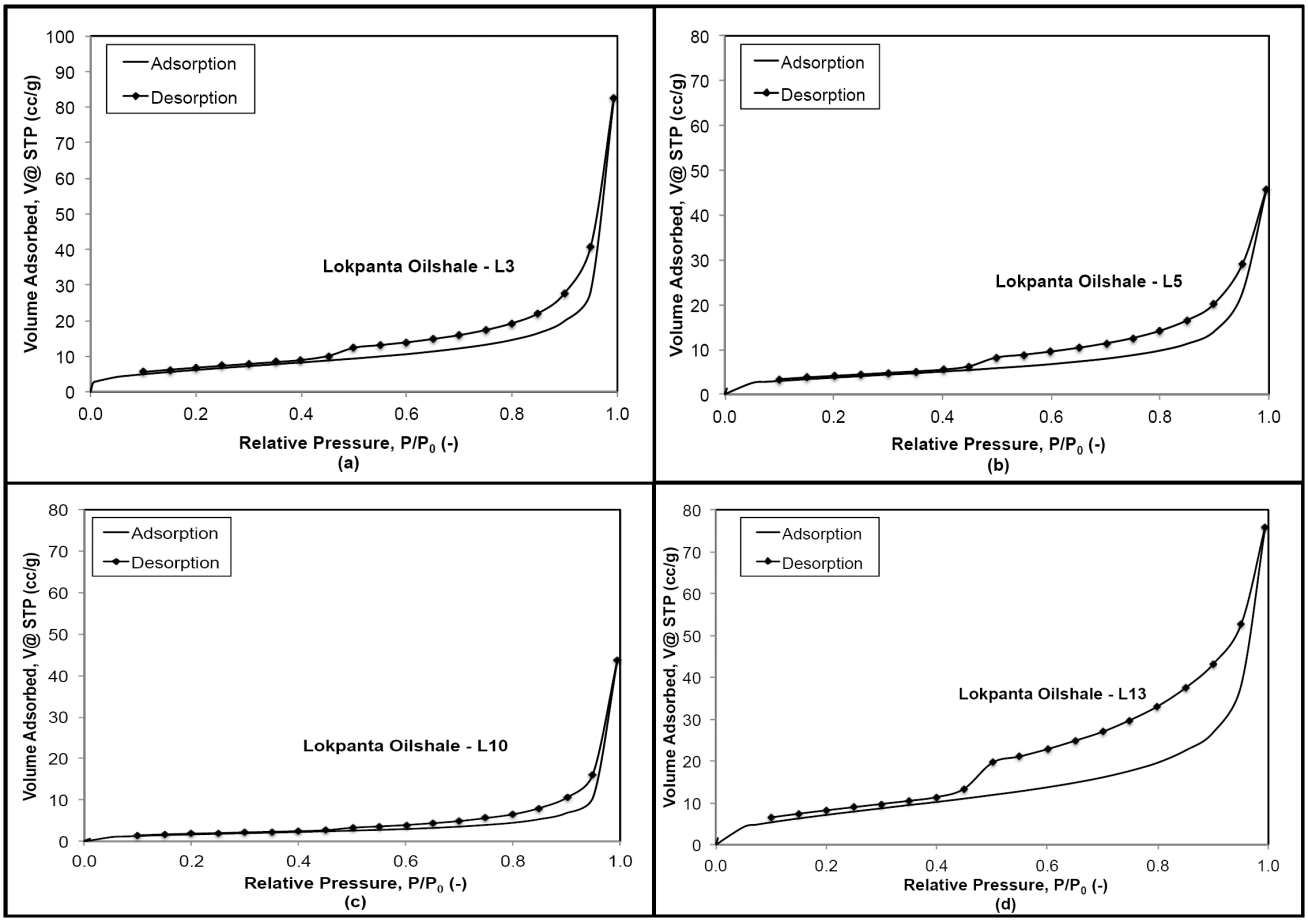

Figure 12—The isotherms of Lokpanta Oilshale: (a) sample L3; (b) sample L5; (c) sample L10; (d) sample L13. The isotherms are similarly shaped and the hystereses of all four samples refer to hysteresis types III for non-rigid aggregates of plate-like particles to silt-shaped particles. Sample L3 and L13 have adsorbed more nitrogen gas than two other samples. This correlates with their large specific surface area.

The isotherms suggest the presence of macropores due to the steep slope at P/P_o=1.0. This is supported by the pore size distributions (Fig. 13) because the increasing trend after 35nm pore width indicates the possible presence of macropores. BET specific surface areas for these samples are consistently larger than Niobrara samples, indicating the possibility of using oil shale reservoirs for storage purposes. The isotherms of L3 and L13 also show a high volume of gas adsorbed, which is accurately reflected by a quantifiable BET specific surface area in Table 1.

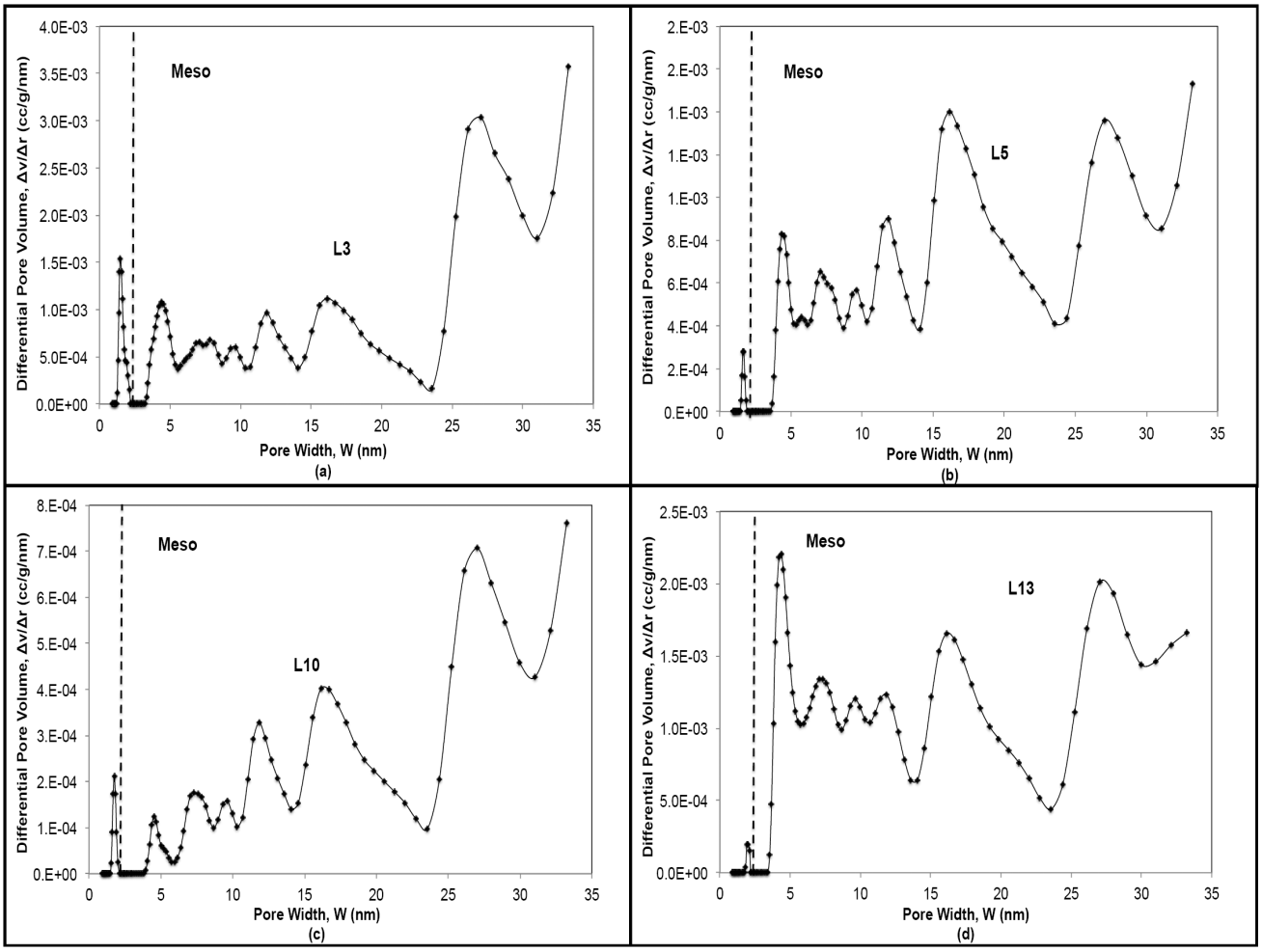

Figure 13—Pore size distribution of Lokpanta oilshale: (a) L3 has some micropores and potentially more macropores; (b) L5 has little micropores, some mesopores and possibly more macropores; (c) L10 has little micropores and an increasing trend of pore sizes; (d) L13 has no micropores, but significant meso- and macro-pores.

Conclusion

Subcritical gas adsorption is essential to intuitively grasp the idea of pore structures in nano-scale. An isotherm maps the whole experiment by recording volume of gas adsorbed and desorbed over the fluid saturation pressure. Overlaying different isotherms together helps comparing pore sizes from micro-, meso- to macropores, and illustrates the occurrence of monolayer coverage and capillary condensation. While isotherms qualitatively present pore textures, quantitative results are available in the form of Brunauer-Emmett-Teller's (BET) specific surface area and Density Functional Theory's (DFT) pore size distribution. From evaluating Niobrara, Hawaiian basaltic rocks, Berea sandstone and Lokpanta oil shale, the importance of cross checking all of the available results has become apparent. Other properties of the sample, such as total organic content, clay content and maturity, help explain some of the structures of pores. When the result does not correlate with available information as expected, some important information on the sample is missing, calling for more tests such as FeSEM.

Almost all isotherms studied in this paper indicate hysteresis type III for non-rigid aggregates of plate-like particles. This is typical of shale nanostructure. While pore geometries are affected by pore size, sorting, packing and clays, studying pore geometry is important in reservoir engineering as it is known to affect data on the water-oil relative permeability curve (Morgan et al 1970). As seen from pore size distribution and isotherms, some of the rocks have significant micropores compared to meso- or macropores. Micropore filling by fluid molecules gives an estimated micropore volume. This is useful in understanding the ability

of micropores to store fluids in the pores by volume instead of adsorbed surface area. Micropore volume and specific surface area of adsorption could be the initial stage in understanding the storage of carbon in CO_2 sequestration.

Acknowledgements

1. This material is based upon the work supported by the U.S. Department of Energy (DOE) National Energy Technology Laboratory (NETL) under the grant number DEFE0023223. This project is managed and administered by the Colorado School of Mines OCLASSH and funded by DOE/NETL and cost-sharing partners.

1. Dr. Manika Prasad, Colorado School of Mines Petroleum Engineering Department
2. Nerine Joewondo, Colorado School of Mines Petroleum Engineering Department
3. Gabriel Unomah, for lending Lokpanta oil shale samples
4. Dr. Andre Revil, for lending Hawaiian basaltic rock samples
5. OCLASSH team, Colorado School of Mines

References

1. Al-Khalifa, A.M., 2016. *Study of the organic content and mineralogy effects on the acoustic properties of the Niobrara Formation, Denver Basin* (Doctoral dissertation, Colorado School of Mines. Arthur Lakes Library).
2. Ambrose, R.J., R.C. Hartmann, M. Diaz-Campos, I.Y. Akkutlu and C.H. Sondergeld. 2012. Shale Gas-In-Place Calculations Part 1: New Pore-Scale Considerations. *SPE Journal*, **17** (1), 219–229.
3. Anovitz, L.M. and Cole, D.R., 2015. Characterization and analysis of porosity and pore structures. *Reviews in Mineralogy and geochemistry*, **80** (1), pp.61–164.
4. Chalmers, G.R., Bustin, R.M. and Power, I.M., 2012. Characterization of gas shale pore systems by porosimetry, pycnometry, surface area, and field emission scanning electron microscopy/transmission electron microscopy image analyses: Examples from the Barnett, Woodford, Haynesville, Marcellus, and Doig units. *AAPG bulletin*, **96** (6), pp.1099–1119.
5. Chapman, H.D., 1965. Cation-exchange capacity. *Methods of soil analysis. Part 2. Chemical and microbiological properties, (methodsofsoilanb)*, pp.891–901.
6. Kang, S.M., Fathi, E., Ambrose, R.J., Akkutlu, I.Y. and Sigal, R.F., 2011. Carbon dioxide storage capacity of organic-rich shales. *Spe Journal*, **16**(04), pp.842–855.
7. Kuila, U., 2013. *Measurement and interpretation of porosity and pore-size distribution in mudrocks: The hole story of shales*. Colorado School of Mines.
8. Kuila, U. and Prasad, M., 2013. Application of nitrogen gas-adsorption technique for characterization of pore structure of mudrocks. *The Leading Edge*, **32** (12), pp.1478–1485.
9. Lowell, S., Shields, J.E., Thomas, M.A. and Thommes, M., 2012. *Characterization of porous solids and powders: surface area, pore size and density.* Springer Science & Business Media, Netherlands. (Vol. **16**).
10. Morgan, J.T. and Gordon, G.T. 1970. Influence of Pore Geometry on Water-Oil Relative Permeability *J. Pet Tech*, pp.199–208
11. Revil, A., Le Breton, M., Niu, Q., Wallin, E., Haskins, E. and Thomas, D.M., 2016. Induced polarization of volcanic rocks–1. Surface versus quadrature conductivity. *Geophysical Journal International*, **208** (2), pp.826–844.
12. Rouquerol, J., Llewellyn, P. and Rouquerol, F., 2007. Is the BET equation applicable to microporous adsorbents?. *Studies in surface science and catalysis*, **160**, pp.49–56.

13. Rouquerol, J., Rouquerol, F., Llewellyn, P., Maurin, G. and Sing, K.S., 2013. *Adsorption by powders and porous solids: principles, methodology and applications*. Academic press.
14. Saidian, M., Godinez, L.J. and Prasad, M., 2016. Effect of clay and organic matter on nitrogen adsorption specific surface area and cation exchange capacity in shales (mudrocks). *Journal of Natural Gas Science and Engineering*, **33**, pp.1095–1106.
15. Sing, K.S., 1985. Reporting physisorption data for gas/solid systems with special reference to the determination of surface area and porosity (Recommendations 1984). *Pure and applied chemistry*, **57** (4), pp.603–619.
16. Storck, S., Bretinger, H. and Maier, W.F., 1998. Characterization of micro-and mesoporous solids by physisorption methods and pore-size analysis. *Applied Catalysis A: General*, **174** (1), pp.137–146.
17. Thommes, M., 2010. Physical adsorption characterization of nanoporous materials. *Chemie Ingenieur Technik*, **82**(7), pp.1059–1073.
18. Thommes, M. and Cychosz, K.A., 2014. Physical adsorption characterization of nanoporous materials: progress and challenges. *Adsorption*, **20**(2-3), pp.233–250.
19. Thommes, M., Kaneko, K., Neimark, A.V., Olivier, J.P., Rodriguez-Reinoso, F., Rouquerol, J. and Sing, K.S., 2015. Physisorption of gases, with special reference to the evaluation of surface area and pore size distribution (IUPAC Technical Report). *Pure and Applied Chemistry*, **87**(9-10), pp.1051–1069.